American Mineralogist, Volume 77, pages 774–783, 1992

Experimental investigation of Fe-Mg distribution between olivine and clinopyroxene: Implications for mixing properties of Fe-Mg in clinopyroxene and garnet-clinopyroxene thermometry

Dexter Perkins

Department of Geology and Geological Engineering, and the Mining and Mineral Resources Research Institute, The University of North Dakota, Grand Forks, North Dakota 58202, U.S.A.

Daniel Vielzeuf

Département de Géologie, Université Blaise Pascal, 5 Rue Kessler, 63038 Clermont-Ferrand, France

Abstract

Experiments conducted in a piston cylinder apparatus at 10.5 kbar, 1000 °C, reveal that the exchange of Fe and Mg between olivine and clinopyroxene is nearly ideal. Fifty-three experimental half-reversals tightly constrain the curve ln K_d vs. Fe/(Fe + Mg). If W_{FaFo} = 4500 J/atom, the weighted least-squares regression of the experimental results yields W_{HdDi} = 3978 ± 423 J/atom and $\Delta G^0_{rxn} = -7208 \pm 174$ J/mol for the exchange reaction. A Monte Carlo regression yields similar results. Fe-Mg mixing in olivine, in the M1 site of clinopyroxene, in garnet, and in orthopyroxene can be characterized by small symmetrical Margules parameters: 4500, 3978, 1590, and 0 J/atom, respectively.

Attempts to perform similar experiments on Fe-Mg exchange between garnet and clinopyroxene were unsuccessful. However, the olivine-clinopyroxene results can be combined with the results of other studies on Fe-Mg exchange between garnet and olivine to calculate a garnet-clinopyroxene thermometer. The calculated thermometer is highly uncertain but yields temperatures 30–190 °C higher than those suggested by some recently published experimental results. One of the recent studies is likely in error; more experimental studies are needed to resolve the discrepancies.

Introduction

Exchange equilibria

The exchange of Fe and Mg between coexisting silicates forms the basis for several important geothermometers, including garnet-biotite (Thompson, 1976; Ferry and Spear, 1978), garnet-clinopyroxene (Ellis and Green, 1979; Pattison and Newton, 1989), garnet-olivine (O'Neill and Wood, 1979; Hackler and Wood, 1989), and garnet-orthopyroxene (Lee and Ganguly, 1988). Exchange equilibria involving garnet are particularly suitable as thermometers because strong partitioning of Fe^{2+} into garnet, relative to other phases, is highly temperature dependent. Recent studies have suggested that in some cases Fe-Mg may reequilibrate well after the peak of metamorphism (e.g., Frost and Chacko, 1989; Pattison and Newton, 1989). In order to evaluate this problem completely, more experimental data on Fe-Mg exchange between coexisting silicates are needed.

In the present study, we have investigated the exchange of Fe and Mg between olivine and clinopyroxene in the CaO-MgO-FeO-SiO_2 system, described by the reaction

$$\underset{\text{½ forsterite}}{\tfrac{1}{2}Mg_2SiO_4} + \underset{\text{hedenbergite}}{CaFeSi_2O_6} = \underset{\text{½ fayalite}}{\tfrac{1}{2}Fe_2SiO_4} + \underset{\text{diopside}}{CaMgSi_2O_6}. \quad (1)$$

The equilibrium constant for this reaction can be calculated as

$$K_{eq} = \frac{a_{Fa}^{1/2} a_{Di}}{a_{Fo}^{1/2} a_{Hd}} \quad (2)$$

where a_{Fa}, a_{Fo}, a_{Di}, and a_{Hd} are activities of fayalite and forsterite in olivine and of diopside and hedenbergite in clinopyroxene. Partitioning of two elements between two phases is more conveniently described in terms of K_d than K_{eq}. For the distribution of Fe and Mg between olivine and clinopyroxene, K_d is

$$K_d = \frac{X_{Fe}^{ol} X_{Mg}^{cpx}}{X_{Mg}^{ol} X_{Fe}^{cpx}}. \quad (3)$$

We were able to obtain tight reversals of K_d for a wide range of Fe/(Fe + Mg) compositions at 10.5 kbar, 1000 °C.

Although, as will be discussed below, Reaction 1 is not particularly suitable as a geothermometer, our experimental results provide valuable information regarding mixing properties of olivine and clinopyroxene solutions. This information can, in turn, be used to calibrate other reactions for application to high-temperature rocks.

Pattison and Newton (1989) have recently investigated

0003–004X/92/0708–0774$02.00

the exchange of Fe and Mg between garnet and clinopyroxene. They studied the reaction

$$\underset{\text{⅓ pyrope}}{\tfrac{1}{3}Mg_3Al_2Si_3O_{12}} + \underset{\text{hedenbergite}}{CaFeSi_2O_6} = \underset{\text{⅓ almandine}}{\tfrac{1}{3}Fe_3Al_2Si_3O_{12}} + \underset{\text{diopside}}{CaMgSi_2O_6}. \quad (4)$$

Pattison and Newton's (1989) results are not completely consistent with several earlier studies (e.g., Ellis and Green, 1979) and suggest that either garnet or clinopyroxene solutions are very nonideal. In addition, many thermometers based on Reaction 4 yield highly variable temperatures, in part because of the many different thermodynamic models that have been employed.

In order to resolve these discrepancies, we sought, as part of this study, to investigate directly the Fe-Mg exchange between garnet and clinopyroxene. Unfortunately, we encountered severe experimental problems involving (1) the synthesis of homogeneous calcium magnesium iron garnets to use as starting material, (2) the growth of pyroxenoid (rather than clinopyroxene) in experimental products, and (3) the difficulty of establishing equilibrium for ternary (calcium magnesium iron) garnets and quaternary (calcium magnesium iron aluminum) clinopyroxene. Because of these problems, we adopted the indirect approach of calculating Reaction 4 by combining our experimental data on Reaction 1 with studies by O'Neill and Wood (1979) and Hackler and Wood (1989) on the exchange of Fe and Mg between garnet and olivine, described by the reaction

$$\underset{\text{⅓ pyrope}}{\tfrac{1}{3}Mg_3Al_2Si_3O_{12}} + \underset{\text{½ fayalite}}{\tfrac{1}{2}Fe_2SiO_4} = \underset{\text{⅓ almandine}}{\tfrac{1}{3}Fe_3Al_2Si_3O_{12}} + \underset{\text{½ forsterite}}{\tfrac{1}{2}Mg_2SiO_4}. \quad (5)$$

Calculating garnet-clinopyroxene Fe-Mg exchange equilibria by combining results of studies on olivine clinopyroxene and garnet olivine avoids many of the complexities of direct experimental investigation. It does, however, introduce large uncertainties, making the resulting thermometer considerably less precise than those derived from direct experimentation.

Thermodynamic models

The conditions of equilibrium for Reaction 1 may be written as follows:

$$-\Delta G^0_{P,T} = RT \ln K_{eq} = RT \ln \frac{a_{Fa}^{1/2} a_{Di}}{a_{Fo}^{1/2} a_{Hd}}. \quad (6)$$

Recall that activities (a_i) are commonly expressed in terms of mole fraction (X_i) and activity coefficient (γ_i). For hedenbergite and diopside, $a_{Hd} = \gamma_{Hd} X_{Hd}$, and $a_{Di} = \gamma_{Di} X_{Di}$. For fayalite and forsterite, $a_{Fa} = (\gamma_{Fa} X_{Fa})^2$, and $a_{Fo} = (\gamma_{Fo} X_{Fo})^2$ because there are two sites for Fe-Mg mixing per formula. These expressions for activity can be substituted into Equation 6, which can then be split into an ideal part, involving K_d, and nonideal parts, involving activity coefficients (γ). For Reaction 1 we obtain

$$\frac{-\Delta G_{P,T}}{RT} = \ln K_d + \ln \frac{\gamma_{Fa}}{\gamma_{Fo}} - \ln \frac{\gamma_{Hd}}{\gamma_{Di}}. \quad (7)$$

There are many activity models that could be chosen for olivine and clinopyroxene. Helffrich and Wood (1989) have presented a cogent discussion of solution models using Margules parameters (W in equations below). For binary and ternary solutions, their equations are consistent with earlier presentations by other authors (e.g., Thompson, 1967; Ganguly and Saxena, 1987).

It should be noted that there is some confusion regarding the use of Margules parameters to calculate activities. Helffrich and Wood's (1989) formalism and the values and equations used here are based on atom units. Other investigators (e.g., Hackler and Wood, 1989) have used mole units. The mixing parameters for olivine used by Hackler and Wood (1989) differ from ours by a factor of 2, equivalent to the octahedral site multiplicity in one olivine formula. Calculated activities are, however, the same because the expressions relating activity and Margules parameters also differ by a factor of 2.

Using an asymmetric model for Fe-Mg olivine we have

$$RT \ln \gamma_{Fa} = X_{Fo}(1 - X_{Fa}) \cdot [W_{FaFo} + 2X_{Fa}(W_{FoFa} - W_{FaFo})]. \quad (8)$$

For symmetric solutions, in which $W_{FaFo} = W_{FoFa}$, Equation 8 simplifies to

$$RT \ln \gamma_{Fa} = X_{Fo}(1 - X_{Fa}) W_{FaFo}. \quad (9)$$

An analogous expression holds for forsterite.

We follow the recommendation of Hackler and Wood (1989) and treat olivine as a symmetric solution. It follows that

$$RT \ln \frac{\gamma_{Fa}}{\gamma_{Fo}} = W_{FaFo}(X_{Fo} - X_{Fa}). \quad (10)$$

Although more complicated solution models have been proposed for clinopyroxene (e.g., Davidson and Lindsley, 1989), we prefer to treat clinopyroxene as a ternary diopside-hedenbergite-wollastonite (Di-Hd-Wo) solution. Choice of these end-members requires that, for binary Hd-Di pyroxenes, $X_{Wo} = 0$. For quadrilateral clinopyroxenes, X_{Wo} has a small negative value, and $X_{Di} + X_{Hd}$ is slightly greater than 1. We assume that the binary joins can be represented as symmetric solutions and that no ternary interaction parameters are needed. It will be shown below that such a model adequately describes our experimental results and is appropriate for discussion of Fe-Mg exchange thermometry in general. Using the equations of Helffrich and Wood (1989), and modifying to take into account our unconventional choice of end-members, we find

$$RT \ln \frac{\gamma_{Hd}}{\gamma_{Di}} = W_{HdDi}(X_{Di} - X_{Hd})\left(\frac{1 + X_{Wo}}{1 - X_{Wo}}\right) + X_{Wo}\Delta W_{Ca} \quad (11)$$

TABLE 1. Synthesis of starting materials

Composition	Experiment no.	P (kbar)	T (°C)	t (h)	Analysis X_{Ca}	Analysis X_{Fe}	Analysis X_{Mg}
$Hd_{100}Di_0$	P89O9	10	1100	14			
cycle 2	P90O9	11	1100	13	48.9(0.5)	51.0(0.4)	0.1(0.1)
$Hd_{90}Di_{10}$	P120N26	10	1100	19			
cycle 2	P122N27	8	1100	21	49.9(0.4)	44.4(1.1)	6.2(1.1)
$Hd_{75}Di_{25}$	P84O7	8	1125	17			
cycle 2	P86O7	8	1125	11	49.8(0.3)	37.5(1.5)	12.7(1.4)
$Hd_{55}Di_{45}$	P83O6	8	1150	6			
cycle 2	P88O8	8	1000	14	49.8(0.3)	27.5(1.4)	22.7(1.2)
$Hd_{40}Di_{60}$	P114N18	7	1150	19			
cycle 2	P117N19	7	1100	14	49.6(0.4)	20.4(0.9)	30.0(1.1)
$Hd_{25}Di_{75}$	P115N18	7	1200	15			
cycle 2	P116N19	7	1250	20	49.9(0.6)	12.0(1.2)	38.2(1.3)
$Hd_{10}Di_{90}$	P121N27	8	1300	4			
cycle 2	P123N28	8	1100	18	50.3(0.5)	5.4(0.7)	44.3(0.9)
Hd_0Di_{100}	UCDI	20	1400	22	49.9(0.2)	0.1(0.1)	50.1(0.2)
$Fa_{100}Fo_0$	UCFAY	20	1400	24	—	99.9(0.1)	0.1(0.1)
$Fa_{90}Fo_{10}$	P49S3	3	1200	8			
cycle 2	P93O11	8	1150	13	—	89.9(0.3)	10.1(0.3)
$Fa_{70}Fo_{30}$	P48S3	3	1250	6			
cycle 2	P92O11	8	1200	8	—	69.7(0.2)	30.3(0.2)
$Fa_{50}Fo_{50}$	P46A30	3	1300	2			
cycle 2	P108N9	6	1200	15	—	49.2(0.5)	50.8(0.5)
$Fa_{30}Fo_{70}$	P110N11	4	1300	4			
cycle 2	P111N12	9	1100	17	—	29.8(0.3)	70.2(0.3)
$Fa_{15}Fo_{85}$	P55S10	4	1275	2			
cycle 2	P112N3	8	1200	23	—	15.2(0.2)	84.8(0.2)
Fa_0Fo_{100}	G100N26	0.001	1400	14			
cycle 2	G101N26	0.001	1400	24	—	0.0	100.0

Note: Compositions in mole percent. Values in parentheses are 1σ. Cycle 2 indicates material recycled (see text).

where the ΔW_{Ca} term is the energetic difference between nonideality of Ca-Fe mixing and Ca-Mg mixing in clinopyroxene (see Appendix 1). The above equations can be combined to yield, for Reaction 1,

$$RT \ln K_d = -\Delta G^0_{P,T} - W_{FaFo}(X_{Fo} - X_{Fa}) + W_{HdDi}(X_{Di} - X_{Hd})\left(\frac{1 + X_{Wo}}{1 - X_{Wo}}\right) + X_{Wo}\Delta W_{Ca}. \quad (12)$$

Note that, given our choice of end-members, X_{Wo} has a very small value for most clinopyroxenes—especially those in our experimental products. Thus, the last term in Equation 12 has only a small effect, as does the coefficient in large parentheses.

Experimental methods

Piston cylinder

Experiments were conducted in a ¾-in. piston cylinder apparatus in the Département de Géologie, Université Blaise Pascal, Clermont-Ferrand, France. Details of the piston cylinder and assembly used for syntheses have been described elsewhere (Perkins and Vielzeuf, 1992).

For reversal experiments, an assembly similar to the one described by Perkins (1983) and Hackler and Wood (1989) was used. The pressure medium was high-Na glass identical to that described by Perkins and Vielzeuf (1992). Starting materials were packed into five holes 1.4 mm in diameter drilled in a graphite disk 2 mm thick. The strength of the assembly, notably the graphite, reduced the pressure being applied to the samples. Calibration experiments, using the reactions ferrosilite = fayalite + quartz (Bohlen and Boettcher, 1982), and fayalite + anorthite = garnet (Bohlen et al., 1983; Perkins and Vielzeuf, 1992), suggested that a correction of $-12 \pm 3\%$ should be applied to all nominal pressures. For our experiments conducted at 12-kbar nominal pressure, actual pressure on the sample was about 10.5 kbar.

Temperature was controlled to ±1 °C using a W26%Re-W5%Re thermocouple. The thermocouple, which intruded into a hole at the center of the graphite disk, was about 1.3 mm from reversal mixtures and at the same vertical level in the assembly. Calibration experiments, using multiple thermocouples, suggested that the sample temperature was the same as that measured by the thermocouple to ±3 °C. Nominal pressure and temperature were reached less than 10 min after an experiment began and were controlled to ±0.3 kbar and ±1 °C during the experiment. At the end of an experiment, quenching to below 300 °C took less than 15 s.

Synthesis of starting materials

Synthetic diopside and fayalite were the same materials used in previous studies (Perkins, 1983; Chatillon-Colinet et al., 1983); all other starting materials were prepared, specifically for this study, from mixtures of high-purity reagents (Fe metal, Fe_2O_3, $CaCO_3$, MgO) and Brazilian quartz. Equimolar amounts of Fe metal and Fe_2O_3 were used in all syntheses. Stoichiometric mixtures

TABLE 2. Cell parameters of starting materials

Composition	a	b	c	β	V
$Hd_{100}Di_0$	9.844(2)	9.030(1)	5.248(1)	104°49(2)′	451.0(1)
$Hd_{90}Di_{10}$	9.826(3)	9.020(2)	5.250(2)	105°01(2)′	449.4(1)
$Hd_{75}Di_{25}$	9.827(4)	9.002(2)	5.252(2)	105°07(2)′	448.6(2)
$Hd_{55}Di_{45}$	9.796(2)	8.982(2)	5.254(1)	105°22(1)′	445.8(1)
$Hd_{40}Di_{60}$	9.788(1)	8.969(1)	5.251(1)	105°32(1)′	444.2(1)
$Hd_{25}Di_{75}$	9.775(2)	8.953(2)	5.254(1)	105°40(1)′	442.7(1)
$Hd_{10}Di_{90}$	9.761(2)	8.942(1)	5.254(1)	105°46(1)′	441.3(1)
Hd_0Di_{100}	9.746(2)	8.949(2)	5.248(1)	105°50(1)′	440.4(1)
$Fa_{100}Fo_0$	4.820(3)	10.477(3)	6.089(2)	—	307.5(2)
$Fa_{90}Fo_{10}$	4.814(1)	10.455(1)	6.079(1)	—	306.0(1)
$Fa_{70}Fo_{30}$	4.806(1)	10.396(2)	6.059(1)	—	302.7(1)
$Fa_{50}Fo_{50}$	4.792(1)	10.337(3)	6.037(3)	—	299.0(1)
$Fa_{30}Fo_{70}$	4.778(1)	10.287(1)	6.017(1)	—	295.8(1)
$Fa_{15}Fo_{85}$	4.766(1)	10.245(2)	6.002(1)	—	293.0(1)
Fa_0Fo_{100}	4.750(1)	10.101(2)	5.981(1)	—	289.9(1)

Note: Units are mole percent, angstroms, degrees, minutes. Values in parentheses are 1σ.

TABLE 3. Starting mixes

Mix	Olivine	Clinopyroxene	Starting ln K_d
A	$Fa_{100}Fo_0$	$Hd_{75}Di_{25}$	$+\infty$
B	$Fa_{70}Fo_{30}$	$Hd_{75}Di_{25}$	−0.25
C	$Fa_{90}Fo_{10}$	$Hd_{55}Di_{45}$	2.00
D	$Fa_{50}Fo_{50}$	$Hd_{55}Di_{45}$	−0.20
E	$Fa_{70}Fo_{30}$	$Hd_{40}Di_{60}$	1.25
F	$Fa_{50}Fo_{50}$	$Hd_{40}Di_{60}$	0.41
G	$Fa_{50}Fo_{50}$	$Hd_{25}Di_{75}$	1.10
H	$Fa_{30}Fo_{70}$	$Hd_{25}Di_{75}$	0.25
I	$Fa_{30}Fo_{70}$	$Hd_{10}Di_{90}$	1.35
J	Fa_0Fo_{100}	$Hd_{10}Di_{90}$	$-\infty$
K	$Fa_{100}Fo_0$	$Hd_{90}Di_{10}$	$+\infty$
L	$Fa_{90}Fo_{10}$	$Hd_{90}Di_{10}$	0.00
M	$Fa_{70}Fo_{30}$	$Hd_{90}Di_{10}$	−1.35
N	$Fa_{15}Fo_{85}$	$Hd_{25}Di_{75}$	−0.64
O	$Fa_{50}Fo_{50}$	$Hd_{10}Di_{90}$	2.20
P	$Fa_{100}Fo_0$	$Hd_{55}Di_{45}$	$+\infty$
Q	$Fa_{70}Fo_{30}$	$Hd_{55}Di_{45}$	0.65
R	$Fa_{30}Fo_{70}$	$Hd_{40}Di_{60}$	−0.44
S	$Fa_{90}Fo_{10}$	$Hd_{40}Di_{60}$	2.60
T	$Fa_{70}Fo_{30}$	$Hd_{25}Di_{75}$	1.95
U	$Fa_{15}Fo_{85}$	$Hd_{04}Di_{96}$	1.44

were prepared for each composition and reacted in graphite capsules (about 10.4 mm in diameter and 9 mm long). Products were reground (incorporating a small amount of graphite) for an hour and packed into slightly smaller graphite capsules for recycling.

After the first synthesis, olivines were nearly homogeneous, containing only minor amounts of unreacted Fe metal and quartz. Recycling eliminated all unreacted material. Microprobe analyses showed olivines to be homogeneous within analytical uncertainty.

Clinopyroxenes were more difficult to make. After some syntheses, X-ray analysis revealed pyroxenoid (ferrobustamite structure) rather than clinopyroxene. For the composition $Hd_{75}Di_{25}$, synthesis required many attempts; formation of pyroxenoid was not always reproducible or consistent. Lindsley (1967) has studied phase relations of $CaFeSi_2O_6$, including the inversion of ferrobustamite to hedenbergite. Our synthesis results are broadly consistent with his study; higher Mg content, higher pressure, and lower temperature favored clinopyroxene formation. Perhaps because of nucleation kinetics, syntheses never produced both clinopyroxene and pyroxenoid in the same charge. In some experiments on $Hd_{75}Di_{25}$ compositions, recycling caused the inversion of pyroxenoid to clinopyroxene or vice versa, even when P-T conditions were the same as in the original synthesis.

After initial clinopyroxene syntheses, heterogeneities of ±10–15% (of amount present) were found for some elements, notably Ca, and several weight percent unreacted material was present. Recycling eliminated unreacted material and homogenized clinopyroxenes considerably, although some heterogeneity was still detected by microprobe analysis.

Synthesis conditions, microprobe analyses and unit-cell parameters are given in Tables 1 and 2. Microprobe analyses all agree well with intended compositions. Most of the synthetic materials were homogeneous to ±1–2 mol%, except for a few intermediate clinopyroxenes that showed heterogeneities on the order of 3%. Unit-cell parameters were refined from slow-scan diffractograms and agree well with previous studies of clinopyroxene (Rutstein and Yund, 1969) and olivine (Fisher and Medaris, 1969). A very small negative volume of mixing is present in both iron magnesium clinopyroxene and olivine solutions. The deviations from ideality are within the 2σ uncertainties of the cell refinements.

Reversal experiments

Reversal experiments, conducted at 1000 °C and 12 kbar of nominal pressure (10.5 kbar after correction for the assembly), were made using mixtures containing one synthetic olivine and one synthetic clinopyroxene (Table 3). The mixtures were ground for 1 h in an agate mortar. After grinding the grains were mostly 3–8 μm in size; 10–20% of the material was finer. Ten to 15 mg of the mixtures were packed into each of the five holes in the graphite disk. Disseminated graphite, left from syntheses, remained at the end of all experiments. It served (along with the graphite capsule) to provide an upper limit for f_{O_2} near magnetite wüstite (French and Eugster, 1965; Perkins and Vielzeuf, 1992). No hint of magnetism was found in any starting or product materials.

Because clinopyroxenes tended to be compositionally zoned unless the charge was very olivine rich, initial experiments were conducted using mixtures of 90 wt% olivine and 10 wt% clinopyroxene. In these experiments, however, large amounts of Ca were lost from clinopyroxene to olivine. The additional degree of compositional freedom made it difficult to determine which compositions represented equilibrium. All subsequent experiments, and the results presented here, were conducted on mixtures of 95 wt% clinopyroxene and 5 wt% olivine.

Microprobe analyses

After a reversal experiment, its products were crushed slightly, half the charge being mounted and polished for microprobe analysis, the other being ground for X-ray diffraction. X-ray diffractograms confirmed that clino-

Table 4. Experimental results at 10.5 kbar, 1000 °C

Mix	Pyroxene X_{Ca}	Pyroxene Fe/(Fe + Mg)	Olivine X_{Ca}	Olivine Fe/(Fe + Mg)	ln K_d
A	0.469	0.784	0.023	0.925	∇1.2288
A	0.451	0.818	0.049	0.929	∇1.0739
A	0.448	0.821	0.026	0.926	∇1.0019
B	0.461	0.675	0.021	0.835	Δ0.8929
B	0.468	0.669	0.020	0.847	Δ1.0092
B	0.466	0.703	0.021	0.860	Δ0.9523
C	0.483	0.613	0.039	0.836	∇1.1714
C	0.486	0.610	0.036	0.821	∇1.0710
C	0.489	0.599	0.038	0.821	∇1.1192
D	0.491	0.467	0.024	0.669	Δ0.8357
D	0.486	0.474	0.023	0.663	Δ0.7802
E	0.468	0.457	0.019	0.677	∇0.9142
E	0.486	0.425	0.016	0.685	∇1.0817
F	0.477	0.363	0.015	0.562	Δ0.8128
F	0.480	0.358	0.014	0.592	Δ0.9543
F	0.480	0.358	0.011	0.530	Δ0.7028
G	0.499	0.261	0.027	0.469	∇0.9171
G	0.478	0.264	0.027	0.469	∇0.8991
G	0.469	0.250	0.023	0.472	∇0.9875
H	0.489	0.213	0.003	0.397	Δ0.8873
H	0.490	0.240	0.005	0.420	Δ0.8319
I	0.476	0.139	0.011	0.272	∇0.8423
I	0.484	0.116	0.006	0.249	∇0.9313
I	0.494	0.116	0.011	0.242	∇0.8926
J	0.469	0.051	0.004	0.101	Δ0.7429
J	0.488	0.047	0.010	0.098	Δ0.7913
J	0.478	0.037	0.008	0.079	Δ0.7920
K	0.413	0.944	0.017	0.979	∇1.0028
K	0.414	0.947	0.019	0.975	∇0.7920
K	0.426	0.942	0.021	0.977	∇0.9796
L	0.443	0.704	0.020	0.856	Δ0.9176
L	0.410	0.865	0.022	0.928	Δ0.6900
L	0.374	0.833	0.014	0.931	Δ0.9988
M	0.419	0.693	0.017	0.829	Δ0.7667
M	0.350	0.674	0.019	0.837	Δ0.9092
M	0.430	0.649	0.019	0.837	Δ1.0197
N	0.453	0.176	0.011	0.334	Δ0.8528
N	0.472	0.180	0.007	0.346	Δ0.8805
O	0.480	0.148	0.008	0.324	∇1.0119
O	0.480	0.178	0.008	0.369	∇0.9958
O	0.453	0.172	0.008	0.344	∇0.9276
P	0.479	0.507	0.028	0.710	∇0.8698
P	0.492	0.562	0.038	0.762	∇0.9143
P	0.494	0.592	0.038	0.762	∇0.7918
Q	0.494	0.504	0.030	0.715	Δ0.9009
Q	0.492	0.562	0.038	0.762	Δ0.9143
R	0.468	0.314	0.029	0.520	Δ0.8612
R	0.476	0.318	0.015	0.518	Δ0.8356
S	0.465	0.529	0.024	0.737	∇0.9165
S	0.463	0.483	0.024	0.729	∇1.0575
S	0.476	0.513	0.028	0.742	∇1.0051
T	0.464	0.359	0.014	0.571	∇0.8678
T	0.414	0.401	0.011	0.651	∇1.0232
U	0.479	0.047	0.003	0.121	∇1.0268
U	0.469	0.053	0.008	0.132	∇1.0033

Note: Mixes A–E, F–J, K–O, and P–U were reacted for 90, 92, 112, and 108 h, respectively. X_{Ca} and ln K_d refer to moles Ca/(Ca + Fe + Mg) and natural log of K_d, respectively, in the products. For uncertainties due to microprobe analyses, see Appendix 2. The symbols Δ (up) and ∇ (down) indicate the direction of change in ln K_d when approaching equilibrium.

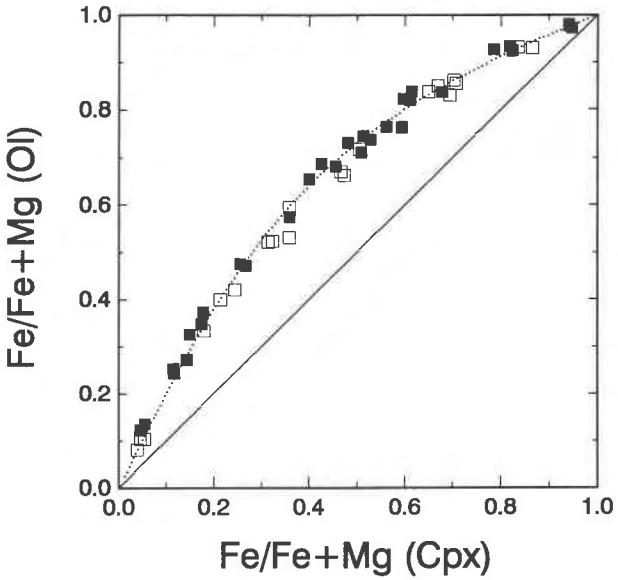

Fig. 1. Fe/(Fe + Mg) in clinopyroxene vs. Fe/(Fe + Mg) in olivine. Open and solid squares are experimental results that converged from low K_d and high K_d values, respectively. The dotted line is a calculated curve for W_{FaFo} = 4500 J/atom, W_{HdDi} = 3978 J/atom, and $\Delta G^0_{rxn1} = -7208$ J/mol. The calculated curve assumes Ca/(Ca + Mg + Fe) in clinopyroxene = 0.475; the experimental points represent variable X_{Ca} amounts.

pyroxene had not inverted to pyroxenoid during any experiments.

Wavelength-dispersive microprobe analyses were obtained using a Cameca Camebax Micro electron microprobe. Analyses were made at 15-kV and 11-nA beam current. Standards were natural silicates and oxides. Analyses were corrected using a standard ZAF program.

No compositional zonation could be detected in the product olivine with a grain size of 10–50 μm. Clinopyroxene, which recrystallized to grains of 10–30 μm, showed noticeable Fe-Mg compositional variability near olivine grains. It was assumed that the clinopyroxene compositions closest to olivine grains represented equilibrium. Fifteen to 30 olivine grains were analyzed in an experimental sample. For each olivine, 5–10 analyses of surrounding clinopyroxene were collected. The several analyses (always at least four) that indicated greatest change of composition were averaged to calculate limits on K_d. Although the greatest amount of reaction was recorded in grain rims, fluorescence and other grain-boundary problems made it necessary to analyze spots at least 3 or 4 μm from olivine-clinopyroxene contacts (cf. Ganguly et al., 1988). Stoichiometric considerations (cation ratios) and analytical totals (deviating markedly from 100 ± 2%) made it clear when an analysis was affected by surrounding grains. Ca analyses in olivine were most problematic—in some cases being strongly influenced by fluorescence of clinopyroxene at distances of 5 μm or more from grain boundaries. It was impossible to detect Ca zonation in the interior of olivine grains because of the small amount present.

Results

Experiments

Tight reversals of K_d were obtained for a wide range of compositions (Table 4) and are shown on a standard composition vs. composition diagram (Fig. 1). In Figure 2, ln K_d is plotted against clinopyroxene composition; it

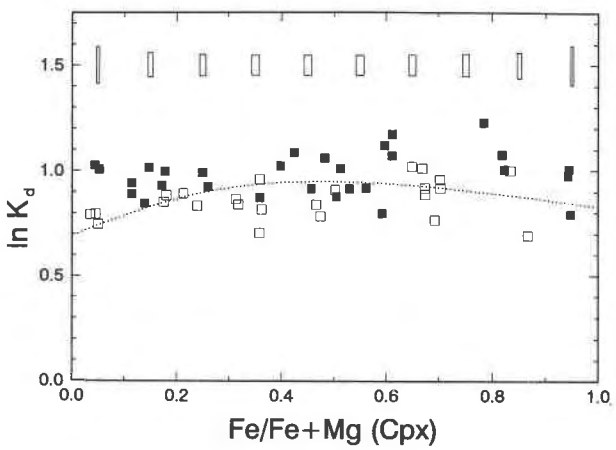

Fig. 2. Values of ln K_d vs. Fe/(Fe + Mg) in clinopyroxene. Experimental data points and calculated curve as in Figure 1. Rectangles at top of diagram show uncertainty (2σ) in X_{Fe} and ln K_d determinations for different X_{Fe} values.

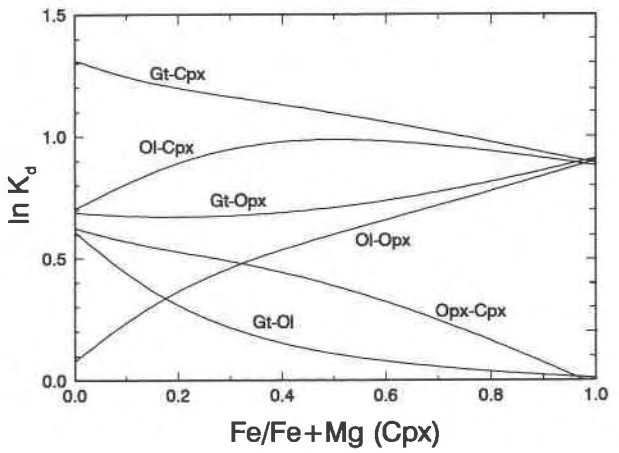

Fig. 3. Calculated ln K_d values for various pairs of iron magnesium silicates at 1000 °C and 10.5 kbar. All values have been normalized to composition of coexisting clinopyroxene. See text for details.

can be seen that almost all compositions yielded ln K_d values between 0.7 and 1.1. With the exception of a few points that appear to have slightly overstepped equilibrium, the half-reversals constrain ln K_d to ±0.05–0.1 over most of the composition range. The ln K_d shows a small decrease from Fe-rich compositions to Mg-rich compositions, indicating that olivine solutions are slightly less ideal than clinopyroxene.

During the experiments, small amounts of Ca moved from clinopyroxene to olivine. Some olivine appeared to gain up to 3 mol% calcium-olivine component, although part of this may result from microprobe convolution effects. Adams and Bishop (1986) obtained experimental reversals on Ca exchange between olivine and clinopyroxene. Our results are consistent with theirs in the composition range they studied [Fe/(Fe + Mg) = 0.15]. Because our experimental samples contained 95% clinopyroxene, most product clinopyroxenes were nearly Ca saturated. The few exceptions (Table 4) are most likely due to heterogeneities in the original reactants. Those grains closest to olivine showed slightly greater Ca loss than grains farther away.

Thermodynamic regression

There are many techniques that could be used to fit Equation 12 to our experimental data. We employed both a Monte Carlo technique, in which each point is treated as a limiting half-bracket, and a weighted least-squares technique. Because of the uniform distribution and smooth variation of the data, both techniques yielded nearly identical results; we report only the least-squares results here. Following Hackler and Wood (1989), we fitted Equation 12 to the data after assuming values for some variables.

Mixing properties of the binary hedenbergite-ferrosilite and diopside-enstatite joins were taken from Davidson and Lindsley (1989) (see Appendices 1 and 3). Hackler and Wood (1989) reviewed that literature and concluded that olivine is essentially a symmetric solution with W_{FeMg} of 4500 ± 1000 J/atom. Using their mean value, our least-squares fit yielded 3978 ± 423 J/atom and −7208 ± 174 J/mol, respectively, for W_{HdDi} and ΔG^0_{rxn1}. A smoothed curve, based on these values, is shown in both Figures 1 and 2 and fits the data well.

We can compare ideality of Fe and Mg mixing in olivine, clinopyroxene, orthopyroxene, and garnet by considering the Margules parameters that would be used in equations such as Equation 9 to calculate activities. On a one-atom basis, of the four silicates, olivine is least ideal and orthopyroxene the most. For olivine, Hackler and Wood's (1989) value (4500 J/atom) is slightly less ideal than the value derived for clinopyroxene in this study (3978 J/atom). For garnet they derived a value of 1590 J/atom, close to ideality. Lee and Ganguly (1988) suggest that Fe-Mg mixing in orthopyroxene is nearly ideal and recommend assuming $W_{FeMg} = 0$. These values are consistent with each other and with the recent experiments cited here, but are highly correlated and may all have to be revised when new experimental data become available. Davidson and Lindsley (1989) have also derived a consistent set of mixing models for orthopyroxene, clinopyroxene, and olivine. It is difficult to compare their results to ours in detail because they used a completely different activity formulation, and there are inconsistencies in their equations. They report W_{FeMg} to be about 3514 J/atom for M1 in clinopyroxene—in excellent agreement with the value derived here.

Fe-Mg fractionation among various silicates

It is possible to combine the experimental results of Lee and Ganguly (1988), Hackler and Wood (1989), and this study to calculate fractionation vs. composition curves in much the same way as is done by isotope geochemists. Figure 3 shows such curves for Fe-Mg fractionation at 1000 °C. The curves, which have all been normalized to coexisting clinopyroxene composition, are metastable be-

cause they apply directly only to Ca-saturated clinopyroxene and Ca-free orthopyroxene, olivine, and garnet. In nature, exchange of Ca adds another dimension that has not been incorporated here. Although not shown, uncertainties of the curves are on the order of ±0.2 log units.

Figure 3 shows that Fe-Mg fractionation among these iron magnesium silicates is compositionally dependent. It is no wonder that earlier experimentalists, who did not consider the effects of Fe/(Fe + Mg) on K_d, obtained some inconsistent results. Nonetheless, the results displayed in Figure 3 are broadly consistent with some earlier experimental studies (e.g., Mori and Green, 1978; Ellis and Green, 1979; Harley, 1984).

Values of ln K_d for garnet clinopyroxene decrease smoothly from about 1.3 (for Mg-rich compositions) to 0.9 (for Fe-rich compositions). In earlier experimental studies, Ellis and Green (1979) found values of about 1.2 at 1000 °C, but they did not consider effects of varying Fe/(Fe + Mg).

Pattison and Newton (1989) obtained ln K_d values between 1.0 and 1.2 for grossular-rich garnets in equilibrium with clinopyroxene at 1000 °C. Their experimental results show a complicated relationship between Fe/(Fe + Mg) and ln K_d, which is not easily explained. If their results are extrapolated to grossular-free garnets, either graphically or using activity models such as that of Berman (1990), they suggest values of about 0.5–0.8, significantly lower than those reported here. The product clinopyroxenes in Pattison and Newton's (1989) experiments were not Ca saturated. Correcting their results to diopside-hedenbergite compositions is problematic, as their results do not accord well with any known activity models for garnet and clinopyroxene. More Ca in clinopyroxene should, however, attract more Fe (because Ca-Fe mixing is more ideal than Ca-Mg mixing). Calculations using equations analogous to Equation 12 show that the effect would be to lower their ln K_d values by another 0.1–0.4 log units, thus increasing the discrepancy farther.

TABLE 5. Thermodynamic data

Phase	S^0	V^0
Fayalite	151.54[A]	46.15[A]
	152.15[B]	
Forsterite	95.51[A]	43.65[A]
	94.10[C]	43.79[C]
Hedenbergite	174.20[D]	67.91[E]
	170.29[F]	68.27[F]
		67.88[I]
Diopside	142.70[G,K]	66.31[E]
	143.09[F]	66.11[H]
	142.50[J]	66.18[J]
Almandine	342.63[B]	115.28[L]
	340.02[J]	115.24[K]
		115.11[J]
Pyrope	266.27[M]	113.13[N,K]
	266.30[K]	113.27[K]
		113.18[J]

Note: Units are J, cc, mole. S^0 and V^0 refer to 1 atm, 298.15 K. Preferred data are given in same row as phase name.

[A] Robinson et al. (1982).
[B] Moecher et al. (1988).
[C] Robie et al. (1978).
[D] Haselton et al. (1987).
[E] This study.
[F] Davidson and Lindsley (1985).
[G] Krupka et al. (1985).
[H] Levien and Prewitt (1981).
[I] Wood (1987).
[J] Berman et al. (1985).
[K] Pattison and Newton (1989).
[L] Holland (1981).
[M] Haselton and Westrum (1980).
[N] Newton and Perkins (1982).

Pressure and temperature effects

Table 5 gives thermodynamic data for olivine and clinopyroxene end-members. From these data we calculate ΔV^0 and ΔS^0 for olivine-clinopyroxene Fe-Mg exchange (Reaction 1) to be −0.35 cc/mol and −3.48 J/mol·K, respectively. Ignoring effects of pressure and temperature on volume and entropy, we can approximate (for units of joules, cubic centimeters, bars)

$$\Delta G^0_{P,T} = \Delta G^0_{P_0,T_0} + \Delta V^0(P - P_0)/10 - \Delta S^0(T - T_0). \quad (13)$$

Combining the ΔV, ΔS, and the ΔG^0 values we derived earlier (−7208 J/mol), we get

$$\Delta G_{\text{rxn}(1),P,T} = 3.48T_K - 0.035P_{\text{bar}} - 11271 \text{ J}. \quad (14)$$

The small pressure coefficient in Equation 14 means that Reaction 1 is practically insensitive to pressure; a change of pressure of 10 kbar results in ln K_d changing by less than 0.1. The temperature coefficient is also small (and would be much smaller if the alternative entropy for hedenbergite listed in Table 5 had been used). A change in temperature of 100 °C will change ln K_d by only about 0.09. Thus, Reaction 1 is unsuitable as a thermometer or barometer, but ideal for experimental investigation of mixing properties because uncertainties in the pressure or temperature of our experiments had little thermodynamic effect.

Garnet-clinopyroxene thermometer

Reaction 4, Fe-Mg exchange between garnet and clinopyroxene, is more suitable as a thermometer. Using data in Table 5, we calculate ΔV^0 and ΔS^0 to be −0.88 cc and −6.05 J/mol·K, respectively. Thus, this reaction is roughly twice as sensitive to temperature and pressure as is Reaction 1.

For Reaction 4, the equation analogous to Equation 6 is

$$\frac{-\Delta G^0_{P,T}}{RT} = \ln K_d + \ln \frac{\gamma_{Al}}{\gamma_{Py}} - \ln \frac{\gamma_{Hd}}{\gamma_{Di}}. \quad (15)$$

We can calculate ΔG^0 for Reaction 4 from values for Reactions 1 and 5. For Reaction 5, Hackler and Wood (1989) determined ΔG^0 at 1000 °C and 1 bar to be −2000 ± 800 J/mol. Making a small correction for pressure, and adding this to ΔG^0 for Reaction 1 (−7208 ± 174 J/mol), we find ΔG^0 for Reaction 4 at 10.5 kbar, 1000 °C, to be

-9768 ± 818 J. We may then derive an equation analogous to Equation 14:

$$\Delta G_{\mathrm{rxn}(3),P,T} = 6.05T_{\mathrm{K}} - 0.088P_{\mathrm{bar}} - 16546 \text{ J}. \quad (16)$$

At 15 kbar, 1000 °C, Equation 15 yields $\Delta G = -11816 \pm 818$ J. Even when the uncertainties are considered, this is 3000–5000 J/mol less than the value derived by Pattison and Newton (1989).

The large uncertainties associated with our calculated Gibbs energy for Reaction 4 translate into large temperature uncertainties ($\approx \pm 150$ °C) if Equation 15 is to be evaluated as a garnet-clinopyroxene thermometer. The uncertainties become even larger because of uncertainties in garnet activity models.

Using Berman's (1990) activity model for garnet, we applied our calibration of the garnet-clinopyroxene thermometer to a variety of samples from high-grade terranes, including those summarized by Pattison and Newton (1989). The resulting temperatures were slightly lower than those calculated using equations of Ellis and Green (1979) and 30–190 °C higher than those calculated using equations of Pattison and Newton (1989). Although the uncertainties are large, the implication of these calculations is that the garnet-clinopyroxene thermometer of Pattison and Newton (1989) may underestimate temperatures of equilibration, even with all the uncertainties involved. This conclusion is in disagreement with that of Green and Adam (1991), who conducted synthesis experiments on glasses prepared from mafic xenoliths.

Unless uncertainties have been greatly underestimated, the three recent experimental studies using synthetic materials (Pattison and Newton, 1989; Hackler and Wood, 1989; this study) are mutually inconsistent. It is not fruitful to speculate on possible problems with the other two studies. If the source of the discrepancy lies with this study, it may involve the lack of complete homogeneity in product clinopyroxenes. More direct experimental studies, especially of garnet-clinopyroxene Fe-Mg exchange, are needed before these important discrepancies can be resolved.

Acknowledgments

The experiments reported in this paper were conducted while D.P. was on a one-year sabbatical at the Département de Géologie, Université Blaise Pascal (Clermont-Ferrand, France). Support came from the Centre National des Récherches Scientifique (contract 90 DBT5-38: Dynamique Globale) and a NATO Senior Scientist Fellowship. This manuscript benefited greatly from discussions with Ariel Provost and Larry Anovitz and from reviews by Tren Haselton and Tom Chacko. Of even more value, however, were the countless hours that John Erjavec spent explaining elementary statistics to a dilettante.

References cited

Adams, G.E., and Bishop, F.C. (1986) The olivine-clinopyroxene geobarometer: Experimental results in the CaO-FeO-MgO-SiO_2 system. Contributions to Mineralogy and Petrology, 94, 230–237.

Berman, R.B. (1990) Mixing properties of Ca-Fe-Mg-Mn garnets. American Mineralogist, 75, 328–344.

Berman, R.B., Brown, T.H., and Greenwood, H.J. (1985) An internally consistent thermodynamic data base for minerals in the system Na_2O-K_2O-CaO-MgO-FeO-Fe_2O_3-Al_2O_3-SiO_2-TiO_2. Atomic Energy of Canada Report, 377, 1–62.

Bohlen, S.R., and Boettcher, A.L. (1982) Experimental investigation and geological applications of orthopyroxene geobarometry. American Mineralogist, 66, 951–964.

Bohlen, S.R., Wall, V.J., and Boettcher, A.L. (1983) Experimental investigation and application of garnet granulite equilibria. Contributions to Mineralogy and Petrology, 83, 52–61.

Chatillon-Colinet, C., Newton, R.C., Perkins, D., III, and Kleppa, O.J. (1983) Thermochemistry of $(Fe^{2+},Mg)SiO_3$ orthopyroxene. Geochimica et Cosmochimica Acta, 47, 1497–1503.

Davidson, P.M., and Lindsley, D.H. (1985) Thermodynamic analysis of quadrilateral pyroxenes. Part II: Model calibration from experiments and applications to geothermometry. Contributions to Mineralogy and Petrology, 91, 390–404.

——— (1989) Thermodynamic analysis of pyroxene-olivine-quartz equilibria in the system CaO-MgO-FeO-SiO_2. American Mineralogist, 74, 18–30.

Ellis, D.J., and Green, D.H. (1979) An experimental study of the effect of Ca upon garnet-clinopyroxene Fe-Mg exchange equilibria. Contributions to Mineralogy and Petrology, 71, 13–22.

Ferry, J.M., and Spear, F.S. (1978) Experimental calibration of the partitioning of Fe and Mg between biotite and garnet. Contributions to Mineralogy and Petrology, 66, 720–732.

Fisher, G.W., and Medaris, L.G. (1969) Cell dimensions and X-ray determinative curve for synthetic Mg-Fe olivines. American Mineralogist, 54, 741–753.

French, B.M., and Eugster, H.P. (1965) Experimental control of oxygen fugacities by graphite-gas equilibrium. Journal of Geophysical Research, 70, 1529–1539.

Frost, B.R., and Chacko, T. (1989) The granulite uncertainty principle: Limitations on thermobarometry in granulites. Journal of Geology, 97, 435–450.

Ganguly, J., and Saxena, S.K. (1987) Mixtures and mineral reactions. Springer-Verlag, New York.

Ganguly, J., Bhattacharya, R.N., and Chakraborty, S. (1988) Convolution effect in the determination of compositional profiles and diffusion coefficients by microprobe step scans. American Mineralogist, 73, 901–909.

Green, T.H., and Adam, J. (1991) Assessment of the garnet-clinopyroxene Fe-Mg exchange thermometer using new experimental data. Journal of Metamorphic Geology, 9, 341–347.

Hackler, R.T., and Wood, B.J. (1989) Experimental determination of Fe and Mg exchange between garnet and olivine and estimation of Fe-Mg mixing properties in garnet. American Mineralogist, 74, 994–999.

Harley, S.L. (1984) An experimental study of the partitioning of Fe and Mg between garnet and orthopyroxene. Contributions to Mineralogy and Petrology, 86, 359–373.

Haselton, H.T., and Westrum, E.F., Jr. (1980) Low temperature heat capacities of synthetic pyrope, grossular, and $pyrope_{60}$-$grossular_{40}$. Geochimica et Cosmochimica Acta, 44, 701–709.

Haselton, H.T., Robie, R.A., and Hemingway, B.S. (1987) Heat capacities of synthetic hedenbergite, ferrobustamite, and $CaFeSi_2O_6$ glass. Geochimica et Cosmochimica Acta, 51, 2211–2218.

Helffrich, G., and Wood, B.J. (1989) Subregular model for multicomponent solutions. American Mineralogist, 74, 1016–1022.

Holland, T.J.B. (1981) Thermodynamic analysis of simple mineral systems. In R.C. Newton, A. Navrotsky, and B.J. Wood, Eds., Thermodynamics of minerals and melts. Springer-Verlag, New York.

Krupka, K.M., Hemingway, B.S., Robie, R.A., and Kerrick, D.M. (1985) High-temperature heat capacities and derived thermodynamic properties of anthophyllite, diopside, dolomite, enstatite, bronzite, talc, tremolite and wollastonite. American Mineralogist, 70, 261–271.

Lee, H.Y., and Ganguly, J. (1988) Equilibrium compositions of coexisting garnet and orthopyroxene: Experimental determinations in the system FeO-MgO-Al_2O_3-SiO_2 and applications. Journal of Petrology, 29, 93–113.

Levien, L., and Prewitt, C.T. (1981) High-pressure structural study of diopside. American Mineralogist, 66, 315–323.

Lindsley, D.H. (1967) The join hedenbergite-ferrosilite at high pressures

and temperatures. Carnegie Institution of Washington Year Book, 65, 230–234.
Moecher, D.P., Essene, E.J., and Anovitz, L.M. (1988) Calculation and application of clinopyroxene-garnet-plagioclase-quartz geobarometers. Contributions to Mineralogy and Petrology, 100, 92–106.
Mori, T., and Green, D.H. (1978) Laboratory duplication of phase equilibria observed in natural garnet lherzolites. Journal of Geology, 86, 83–97.
Newton, R.C., and Perkins, D. (1982) Thermodynamic calibration of geobarometers based on the assemblages garnet-plagioclase-orthopyroxene (clinopyroxene)-quartz. American Mineralogist, 67, 203–222.
O'Neill, H.St.C., and Wood, B.J. (1979) An experimental study of Fe-Mg partitioning between garnet and olivine and its calibration as a geothermometer. Contributions to Mineralogy and Petrology, 70, 59–70.
Pattison, D.R.M., and Newton, R.C. (1989) Reversed experimental calibration of the garnet-clinopyroxene Fe-Mg exchange thermometer. Contributions to Mineralogy and Petrology, 101, 87–103.
Perkins, D. (1983) The stability of Mg-rich garnet in the system CaO-MgO-Al_2O_3-SiO_2 at 1000–1300 °C and high pressure. American Mineralogist, 68, 355–364.
Perkins, D., and Vielzeuf, D. (1992) Reinvestigation of fayalite + anorthite = garnet. Contributions to Mineralogy and Petrology, in press.
Robie, R.A., Hemingway, B.S., and Fisher, J.R. (1978) Thermodynamic properties of minerals and related substances at 298.15 K and 1 bar (10^6 pascals) pressure and at higher temperatures. U.S. Geological Survey Bulletin 1452, 1–456.
Robinson, G.R., Jr., Haas, J.L., Jr., Schafer, C.M., and Haselton, H.T., Jr. (1982) Thermodynamic and thermophysical properties of selected phases in the systems MgO-SiO_2-H_2O-CO_2, CaO-Al_2O_3-SiO_2-H_2O-CO_2, and Fe-FeO-Fe_2O_3-SiO_2 chemical systems, with special emphasis on the properties of basalts and their mineral components. U.S. Geological Survey Open File Report 83-79.
Rutstein, M.S., and Yund, R.A. (1969) Unit-cell parameters of synthetic diopside-hedenbergite solid solutions. American Mineralogist, 54, 238–245.
Thompson, A.B. (1976) Mineral reactions in pelitic rocks: II. Calculation of some P-T-X(Fe-Mg) phase relations. American Journal of Science, 276, 425–454.
Thompson, J.B., Jr. (1967) Thermodynamic properties of simple solutions. In P.H. Abelson, Ed., Researches in geochemistry, vol. 2, p. 340–361. Wiley, New York.
Wood, B.J. (1987) Thermodynamics of multicomponent systems containing several solid solutions. In Mineralogical Society of America Reviews in Mineralogy, 17, 71–95.

Manuscript received July 24, 1991
Manuscript accepted March 13, 1992

Appendix 1. Ca-Mg and Ca-Fe mixing in clinopyroxene

For binary hedenbergite-ferrosilite and diopside-enstatite solutions, the excess Gibbs energy of mixing (ΔG^{xs}) can be described using an asymmetric Margules formulation (Davidson and Lindsley, 1989):

$$\Delta G^{xs}_{Hd\text{-}Fs} = (W_{Hd}X_{Fs} + W_{Fs}X_{Hd})X_{Hd}X_{Fs} \quad (A1)$$

$$\Delta G^{xs}_{Di\text{-}En} = (W_{Di}X_{En} + W_{En}X_{Di})X_{Di}X_{En} \quad (A2)$$

where, in units of joules/atom and bars, $W_{Hd} = W_{FeCa} = 20001 + 0.0271P$, $W_{Fs} = W_{CaFe} = 18682 - 0.0864P$, $W_{En} = W_{CaMg} = 26125 - 0.0384P$, and $W_{Di} = W_{MgCa} = 32301 - 0.0067P$. Following Helffrich and Wood (1989), the ΔW_{Ca} term in Equation 12 is, then,

$$\Delta W_{Ca} = \tfrac{1}{2}W_{Fs}(1 + X_{Wo} - 2X_{Hd}) + \tfrac{1}{2}W_{Hd}(1 - X_{Wo} + 2X_{Hd}) - \tfrac{1}{2}W_{En}(1 + X_{Wo} - 2X_{Di}) - \tfrac{1}{2}W_{Di}(1 - X_{Wo} + 2X_{Di}). \quad (A3)$$

This term is not very significant for the pyroxenes in the experimental products because they are nearly Ca saturated. It has a value of 300–800 J/mol for most of the experimental compositions.

Appendix 2. Evaluating imprecision due to microprobe analyses

It is difficult to evaluate all the sources of uncertainty in the experiments. With the assumption that there are no complications involving attainment of equilibrium, errors due to the imprecision of microprobe analyses appear to be by far the most significant. Calculating uncertainties (σ) in $X_{Fe}/(X_{Fe} + X_{Mg})$ and K_d is complicated by correlations among variables. Consider two correlated variables, X and Y, with a correlation coefficient of ρ_{XY}. Define two functions of X and Y, $R = X/Y$ and $S = X/(X + Y)$. It can be shown that uncertainty in R and S can be estimated by

$$\frac{\sigma_R^2}{R^2} = \frac{\sigma_X^2}{X^2} + \frac{\sigma_Y^2}{Y^2} - 2\rho_{XY}\left(\frac{\sigma_X\sigma_Y}{XY}\right) \quad (A4)$$

$$\frac{\sigma_S^2}{S^2} = \frac{\sigma_X^2 Y^2}{(X + Y)^2X^2} + \frac{\sigma_Y^2}{(X + Y)^2} - \frac{2Y\sigma_X\sigma_Y\rho_{XY}}{(X + Y)^2X}. \quad (A5)$$

For our purposes, let $X = X_{Fe}$ and $Y = X_{Mg}$ (in either olivine or clinopyroxene). These mole fractions can be calculated from microprobe analyses. The correlation coefficient between X and Y, ρ_{XY}, is approximately -1 because the sum of X and Y must be a constant. The imprecision of an analysis for any element is calculated from the number of X-ray counts (N). The uncertainty in X can be found from

$$\frac{\sigma_X}{X} = \frac{\sqrt{N}}{N}. \quad (A6)$$

An analogous expression holds for Y.

Uncertainty in $X_{Fe}/(X_{Fe} + X_{Mg})$ can be found by evaluating Equation A5 for either olivine or clinopyroxene. Uncertainty in K_d is a two-step process. First, the uncertainty of X_{Fe}/X_{Mg} is found for both olivine and clinopyroxene, using Equation A4. Then these values are combined using Equation A4 again, but noting that errors in analyses of clinopyroxene and olivine are not correlated, to get the uncertainty in K_d. This value in turn is used to calculate uncertainty in ln K_d. For thermodynamic regressions, each data point was weighted according to the inverse square of imprecision in ln K_d.

Appendix 3. Least-squares regression

It is not possible to regress Margules parameters for the hedenbergite-ferrosilite and diopside-enstatite joins from the experimental data because the data only encompass a narrow range of X_{Wo} values. We assumed mixing on those joins behaved as reported by Davidson and Lindsley (1989) (see Appendix 1) in order to regress values for the other three variables. Marginal standard deviations were still large because of correlations between W_{FaFo} and W_{HdDi} ($\rho > 0.98$). Values of W_{FaFo} between -17000 and $+21000$ J/atom (corresponding to W_{HdDi} and ΔG^0_{rxn1} values of about -17800 to $+20680$ J/atom and -16500 to $+3040$ J/mol, respectively) all fit to $\pm 1\sigma$. We therefore adopted the approach of assuming values for W_{FaFo}, in addition to W_{HdFs} and W_{DiEn}, in order to regress the other two variables (cf. Hackler and Wood, 1989).

Equation 12 may be rewritten:

$$Y = A_1 + A_2Z \quad (A7)$$

where

$$Y = RT \ln K_d - X_{Wo}(W_{HdWo} - W_{DiWo}) + W_{FaFo}(X_{Fo} - X_{Fa}) \quad (A8)$$

$$Z = (X_{Di} - X_{Hd})(1 + X_{Wo})/(1 - X_{Wo}) \quad (A9)$$

$$A_1 = -\Delta G_{rxn(1)} \quad (A10)$$

$$A_2 = W_{HdDi}. \quad (A11)$$

We then define a matrix, X, that has one row for each of the N observations:

$$X = \begin{vmatrix} 1 & Z_1 \\ 1 & Z_2 \\ \cdot & \cdot \\ 1 & Z_N \end{vmatrix}. \quad (A12)$$

We also define the weighting matrix, W, that is a diagonal $N \times N$ matrix. The nondiagonal terms are 0, the diagonal terms are given by

$$W_{ii} = 1/\sigma_i^2 \quad (A13)$$

where σ_i is the uncertainty of any measurement. In this study the only source of uncertainty considered was that generated by analytical imprecision (see Appendix 2).

The best-fit values for A_1 and A_2 are found in vector **A** by:

$$\mathbf{A} = (X^T W X)^{-1} X^T W Y. \quad (A14)$$

Correlation coefficients and standard deviations may be calculated from the variance-covariance matrix, found by

$$V = (X^T W X)^{-1} \sigma_{fit}^2 \quad (A15)$$

where σ_{fit} is the standard deviation of the fit. Typical results of the regressions are given in Appendix table 1.

Although yielding the lowest σ_{fit}, the best-fit values of 2585, 2036, and −8033 are not significantly more probable than the others. Hackler and Wood (1989), however, have suggested that W_{FaFo} is about 4500 J/atom. If that value is accepted, then the regression yields $W_{HdDi} = 3978 \pm 423$ J/atom and $\Delta G^0_{rxn1} = -7208 \pm 174$ J/mol. Correlation between the two variables is −0.295.

The calculated curve actually fits the data better than is obvious from Figure 2 because the curve in Figure 2 was calculated for constant X_{Wo}. If $\pm 1\sigma$ is considered (see Appendix 2), the calculated curve is only inconsistent with two of the 53 half-reversals. Within 2σ, it agrees with all of them. It should be pointed out that the σ_{fit} values given below overestimate the error by about a factor of 2. They were calculated without considering the direction of approach (increasing or decreasing ln K_d) to equilibrium.

Appendix table 1. Results of regression

W_{FaFo}	W_{HdDi}	ΔG^0_{rxn1}	σ_{fit}
−10000	−10726	−13458	1948
−5000	−5656	−11303	1562
0	−585	−9147	1326
2585	2036	−8033	1292
4500	3977	−7208	1311
5000	4484	−6992	1322
10000	9555	−4836	1552

Note: Units are J/atom for Margules parameters, J/mol for ΔG^0_{rxn1}.